Influence of SiO_2/Al_2O_3 Stoichiometry on Mullite Formation: Synthesis and Characterization via Solid State Reaction

Sukaina Sahib Mohammed[1], Fezaa Shala neda[1] and Jafer Fahdel Odah[2]

[1,2]*Department of Medical Physics, College of Medicine, Al Mustansiriiyah University.*

[2]*Department of Medical Physics, College of Science, Al-Karkh University of Science.*

[*]*Corresponding Author: sukainsahib@uomustansiriyah.edu.iq*

Received 11 Nov. 2025, Accepted 13 Dec. 2025, published 30 Dec. 2025.
DOI: 10.52113/2/12.02.2025/227-245

Abstract This study investigates the effect of varying SiO_2/Al_2O_3 weight ratios on mullite formation synthesized through a solid-state reaction route. Four samples were prepared using different alumina–silica weight ratios: S1 (2.8 g SiO_2, 7.2 g Al_2O_3), S2 (4.7 g SiO_2, 5.3 g Al_2O_3), S3 (6.4 g SiO_2, 3.6 g Al_2O_3), and S4 (3.7 g SiO_2, 6.3 g Al_2O_3), with each batch weighing 10 g. The mixed powders were calcined at 900 °C to remove moisture and impurities, followed by sintering at 1350 °C to promote mullite crystallization. X-ray diffraction confirmed the formation of the orthorhombic 3:2 mullite phase, and crystallite sizes were calculated using the Scherrer equation. SEM images showed that increasing SiO_2 content enhanced the development of elongated acicular grains due to a transient silica-rich liquid phase and increased Al–Si interdiffusion. Among the prepared compositions, S4 exhibited the highest mullite purity and most developed grain structure. This study demonstrates a simple and cost-effective approach for optimizing mullite synthesis for industrial applications.

***Keywords*:** Mullite, Solid state reaction, sintering temperature, Alumina, Silica system, structural properties.

1. Introduction

Mullite is an intermediate phase in the Al_2O_3:SiO_2 system that can exist under atmospheric pressure [1, 2]. Mullite's crystal structure is commonly an orthorhombic aluminosilicate system composed of $Al_2(Al_2+2xSi_{2-2x})O_{10-x}$ [3, 4]. In general, the mullite structure consists of chains of AlO_6 octahedra at the margins and center of the unit cell. These chains grow in the direction of *c*-axis. They connect by double chains of (Al, Si) O_4 tetrahedra parallel to the c-axis. Mullite is extremely rare in nature due to its creation circumstances, which include high temperatures and low pressure [5, 6]. Despite its scarcity as a naturally occurring, mullite has become as an essential phase found in conventional and sophisticated ceramics [7]. Mullite rose to prominence in the 1970s due to its exceptional qualities [8]. Considerable amount of interest in mullite is given in contemporary oxide ceramics due to its unique characteristics [9]. The use of mullite in a

variety of sectors piques researchers' interest in conducting a comprehensive study of mullite and mullite-based composites using numerous synthetic processes. Mullites are chemically synthesized since they are scarce in nature [10]. A wide range of synthetic strategies were used for preparing mullite. Mostly, they depend on heating stoichiometric proportions of an alumina/silica mixture. The difference between these strategies is the main source of these oxides [11].

Mullite requires a high temperature and low pressure conditions for its formation [12, 13]. Practically, a synthesis process is needed for its production. There are three fundamental routes for its synthesis, which are: sintering, melting, and chemical processing [14]. The most often utilized techniques for mullite production is solid-state process [15, 16]. This process consists of two necessary steps. Firstly, the alumina and silica mixture must be heated to a temperature below its melting point. Then, the mixture is left to be crystallized and densified into the phase. Liquid-state synthesis, on the other hand, includes heating mixtures higher than their melting point and then cool it for phase crystallization [17, 18].

In this study, mullite is synthesized through solid state reaction of silica and alumina powders with altered weight ratios, tailed by high-temperature sintering. The structural analysis and phase identification of the synthesized samples is performed using X-ray diffraction (XRD). Scanning electron microscopy (SEM) is used for microstructural analysis. The aim is to investigate the influence of silica-to-alumina weight ratio on mullite phase development and to determine the optimal conditions for producing high-purity mullite through a cost-effective.

Although many studies have discussed mullite synthesis [19, 20], the effect of non-stoichiometric SiO_2/Al_2O_3 weight ratios prepared strictly through the solid-state route remains insufficiently addressed. The novelty of the present work lies in examining how deviations from the ideal ratio influence mullite crystallization, crystallite size, and microstructural evolution. This study also provides a clearer understanding of the relationship between SiO_2 content, liquid-phase formation, and anisotropic grain growth. Unlike chemical or sol–gel methods, this work focuses on a practical and cost-effective process that can be scaled for industrial applications [21, 22].

2. Methodology (Experimental Procedure)

Mullite samples were prepared using the solid-state reaction method by mixing different weight ratios of both alumina and silica. The final samples were labeled as S1 (SiO_2: 2.8 g

and Al_2O_3: 7.2 g), S2 (SiO_2: 4.7 g and Al_2O_3: 5.3 g), S3 (SiO_2: 6.4 g and Al_2O_3: 3.6 g), and S4 (SiO_2: 3.7 g and Al_2O_3: 6.3 g), with each sample weighing 10 g.

The mass of 10 g was selected to ensure homogeneous mixing and to provide sufficient material for XRD, SEM, and EDS characterization.

Deionized water was added to all samples, which were then left for 48 hours to allow proper cohesion of the powders. The mixtures were then stirred using a magnetic stirrer for 6 hours without heating, and their pH was adjusted to pH = 9.

The mixed oxides were dried in an oven at 100 °C for 60 minutes. After drying, the powders were calcined at 900 °C for 2 hours to remove moisture and impurities. The calcined powders were then pressed into pellets using a hydraulic press at a pressure of 12 tons for 1 minute. These pellets were then sintered at 1250 °C for 4 hours and subsequently characterized by XRD, SEM, and EDS to determine their phase composition, morphology, and elemental structure

3. Results and Discussion

The beginning material and processing of mullite are connected to its microstructure and subsequent qualities, and a basic processing approach is used to produce mullite with appropriate microstructure and mechanical properties. The phase composition of every sample series as a function of sintering temperature is determined by XRD analysis (fig. 1).

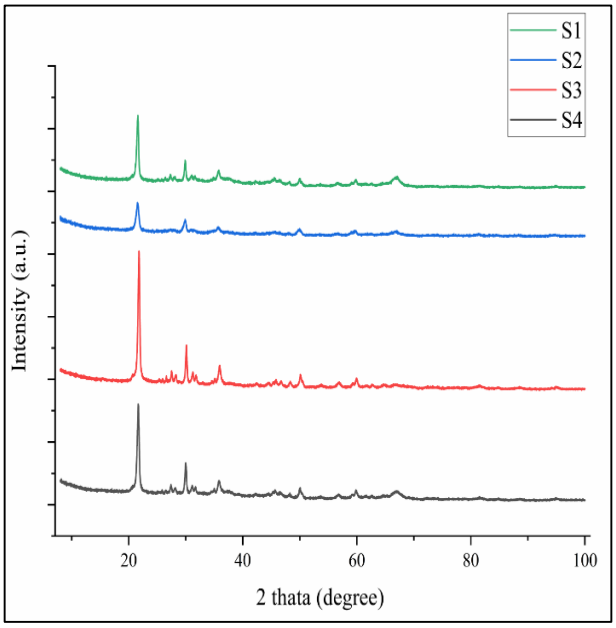

Figure (1): XRD pattern for mullite synthesized using solid state sintering reaction.

The phase composition of the samples sintered at 1250 °C was examined by XRD, as shown in Figure (1). The calcination step at 900 °C served only to remove moisture and volatile impurities, as mullite formation does not occur at temperatures below ~1200 °C. After sintering at 1250 °C, all samples exhibited high-intensity diffraction peaks corresponding to orthorhombic 3:2 mullite.

A dense orthorhombic mullite phase was identified with characteristic peaks at 2θ = 21.3° (110) and 23.9° (120), matching JCPDS

card No. 15-0776. Peaks belonging to α-Al_2O_3 appeared at 35.2° (104), 43.3° (113), 52.5° (024), and 57.5° (116), consistent with JCPDS card No. 46-1212. A broad hump around 20° indicated the presence of an amorphous silica phase.

To enhance the analysis, the crystallite size of the mullite phase was calculated using the Scherrer equation, and the results confirmed that crystallinity improves as the SiO_2/Al_2O_3 ratio approaches the optimal composition.

The mullite crystals produced by the solid state sintering process are acicular or equiaxial in shape and range in size from 1 to 100 µm. Micrographs of mullite crystals produced by solid-state sintering operations are displayed in Figure (2). To determine the materials' microstructure, scanning electron microscopy using an energy dispersive spectrometer (EDS) was used silica, the interior portion is thought to be rich in alumina [23].

To provide a more quantitative description of crystallinity, the crystallite size of the mullite phase was calculated using the Scherrer equation (equation 1), as recommended by the reviewer. The equation is expressed as:

$$D = \frac{K\gamma}{\beta COS\theta} \qquad (1)$$

where:

- D is the crystallite size,
- K is the shape factor (0.9),
- λ is the X-ray wavelength (1.5406 Å for Cu–Kα),
- β is the full width at half maximum (FWHM) of the selected peak (in radians),
- θ is the Bragg diffraction angle.

The (120) mullite peak was selected for the calculation due to its intensity and clarity. The obtained values showed that the crystallite size increases gradually with higher SiO_2 content, which agrees with the observed grain coarsening in the SEM images.

The SEM pictures show that the shape of the materials is influenced by the silica concentration and source. The particles in the mullite samples look separated as the weight ratio of silica increases Figure (2 C), and the grain sizes appear to rise for all samples sintered at 1350 °C.

However, when the silica weight declined, the samples displayed well-developed grains, which are linked to the silica phase; sample S_4 contains a larger number of these grains than the samples that include them. An alteration to the mullite ceramics microstructure was observed when $SiO_2$was added [24]. The grains changed from columnar shape to long rod shape.

Every sample has a low residual porosity and a dense microstructure. The sub-amorphous mullite component grains in these materials' microstructure do not exhibit any preferred orientation or direction. Al, O, and Si are among the elements that are almost stoichiometric to mullite. As seen in Figure 3, the mullite grain size increases and the grain boundary becomes fuzzy when 4.7 g of SiO_2 is added.

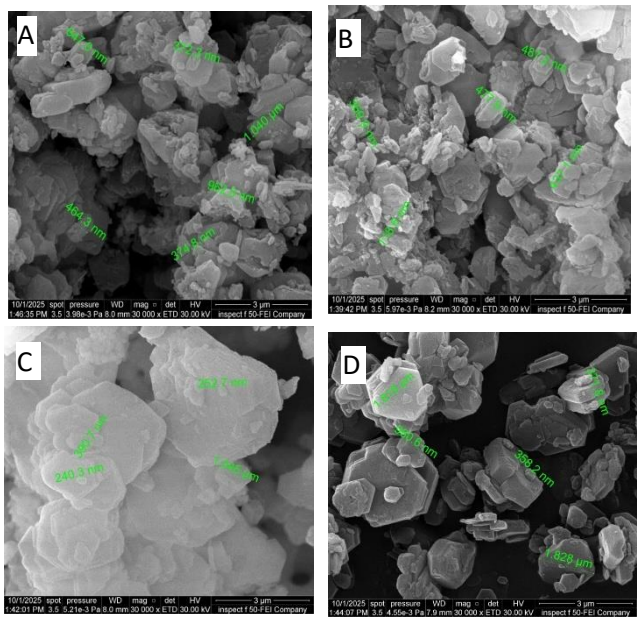

Figure (2): SEM images for mullite synthesized using solid state reaction, where A stands for S1, B for S2, C for S3 and D for S4

The anisotropic development of mullite is evident when the SiO_2 concentration is raised to 6.4 g; in the meantime, the plates thicken. As was previously mentioned, solid solutions were formed when Si^{4+} ions were added to mullite at high temperatures. The substitution of Al^{3+} with Si^{4+} led to a reduction in the activation energy of ion diffusion. These results align to published report in [25]. The EDX spectrum of these specimens, which are shown in Figure (3), revealed the presence of iron, one of the primary constituents of mullite, along with the key elements Al, Si, and O. The mullite phase production is demonstrated by the EDX analysis result, which is in agreement with the XRD analysis.

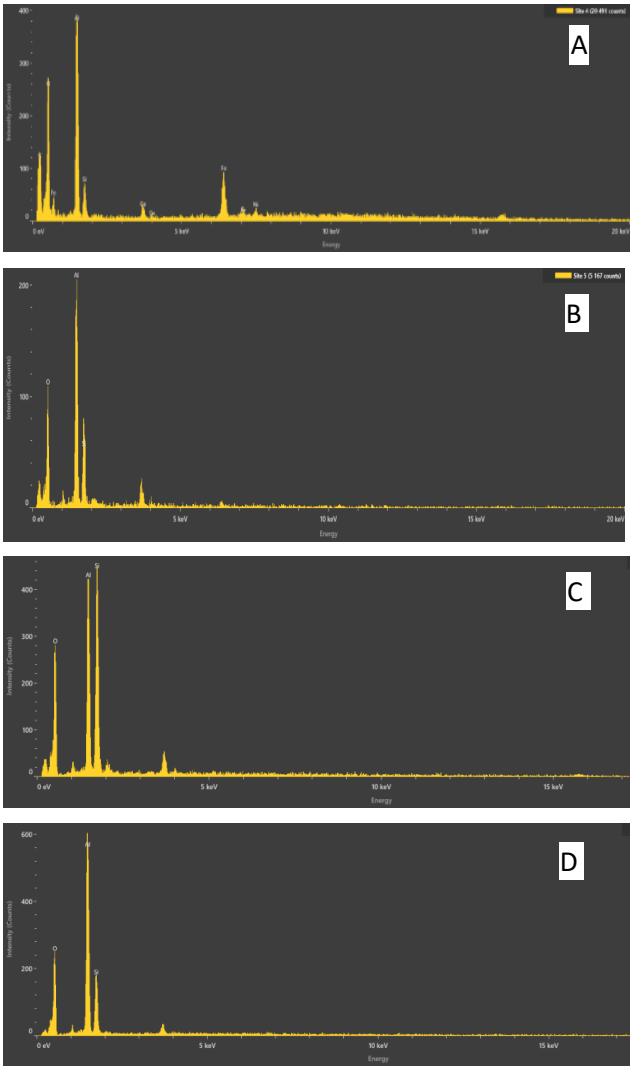

Figure (3): EDS for mullite synthesized using solid state

reaction, where A stands for S1,B for S2,C for S3 and D for S4

The current mullite phase's production process can be attributed to the inter-diffusion of silicon and aluminum ionic species in the alumina–silica contact zone at high calcination temperatures.

4. Conclusion

The results of this study showed that varying the SiO_2/Al_2O_3 weight ratios has a clear influence on mullite formation, microstructure, and crystallinity when using the solid-state reaction method. XRD analysis confirmed the presence of the orthorhombic 3:2 mullite phase in all samples after sintering at 1350 °C, along with small peaks related to α-Al_2O_3 and a broad hump indicating the presence of an amorphous silica phase. The crystallite size calculated using the Scherrer equation showed a gradual increase with increasing SiO_2 content, in agreement with the microstructural observations.

SEM images revealed that samples with higher SiO_2 content tended to form elongated acicular grains, due to the presence of a transient SiO_2-rich liquid phase that enhanced Al–Si interdiffusion. In contrast, samples with lower SiO_2 showed more compact and well-developed equiaxed grains. This demonstrates the strong relationship between the SiO_2/Al_2O_3 ratio and the grain morphology of mullite. EDS analysis confirmed the presence of Al, Si, and O as the main components of the mullite structure, while the small amount of Fe observed originated from raw-material impurities rather than from the mullite phase itself.

Overall, sample S4 produced the highest mullite purity and best-developed grain structure, indicating that this composition is the most suitable among the tested ratios for achieving improved mullite formation through the solid-state method.

Credit Author Contributions Statement:

Fezaa Shala Neda: Supervision, Guidance in Medical Physics Aspects, and Manuscript Reviewing and Editing.
Jafer Fahdel Odah: Co-Supervision Validation, Resources, and Final Review of the Manuscript.

Funding Statement:
This paper received no specific grant from any funding agency in the public, commercial, or not-for-profit sectors.

Data availability statement:
The data supporting the findings of this study are available from the corresponding author upon reasonable request.

Conflict of Interest Statement:

The authors declare that there is no conflict of interest regarding the publication of this paper.

Ethical Approval: Not applicable.

Informed Consent: Not applicable.

Acknowledgment

The authors would like to express their sincere gratitude to the Laboratory of the University of Al-Karkh for providing the necessary facilities and material to carry out this research. The authors also acknowledge the support of the Research and Development Authority for enabling the required testing an analysis.

References

[1] Lima, L.K.S., Silva, K.R., Menezes, R.R., Santana, L.N.L.; Lira, H.L., 2022, Microstructural characteristics, properties, synthesis and applications of mullite: A review, Ceram. 68, 126–142.

[2] Roy, J., Bandyopadhyay, N., Das, S.;, Maitra, S., 2011, Studies on the Formation of Mullite from Diphasic Al_2O_3-SiO_2 Gel by Fourier Transform Infrared spectroscopy, Iran. J. Chem. Chem. Eng. 30(1).

[3] Schneider, H., Fischer, R., Schreuer, J. J. Am., 2015, Mullite: Crystal Structure and Related Properties, Ceram. Soc. 98(10), 2948–2967.

[4] Rout, P.K., Das, D., Roy, R., Rout, P.K., 2021, A review of advanced mullite ceramics, Eng. Sci. 18, 20–30

[5] Romero, M., Padilla, I., Contreras, M., López-Delgado, A., 2021, Mullite-Based Ceramics from Mining Waste: A Review, Minerals 11, 332.

[6] Choo, T.F., Mohd Salleh, M.A., Kok, K.Y., Matori, K.A., 2019, A Review on Synthesis of Mullite Ceramics from Industrial Wastes, Recycling 4, 39.

[7] Roy, R., Das, D., Rout, P.K., 2022, A Review of Advanced Mullite Ceramics, Eng. Sci. 18, 20–30.

[8] Peng, B., Ding, X., Zhao, Y., Deng, X., Wang, D., Jin, X., Ran, S., 2023, J. Mater. Res. Technol., 24.

[9] Mahdi, S.H., Saad, K.A., Kanbur, U., 2024, Effect of Adding Al_2O_3 on Some Physical Properties of the Ceramic Compound.

[10] Nair, S.G., Sreejith, K.J., Srinivas, C., Prabhakaran, K., Devasia, R., 2022, Low temperature mullite forming pre-ceramic resins of high ceramic yield for oxide matrix composites, Ceram. Int. 48(13),

[11] Badanoiu, A.-I., Stoleriu, S.-P., Carocea, A.-C.; Trusca, R. 2025, Influence of Synthesis Route on Composition and

Main Properties of Mullite Ceramics Based on Waste, Materials, 18(5), 1098

[12] Chen, Y., Tian, X., Su, K., Wang, Y., Liu, X., Zhao, F. 2023, Preparation and properties of porous mullite‐based ceramics fabricated by solid state reaction, Ceram. Int. 49(19).

[13] Carrizosa, R., De Noni Jr., A., López-Delgado, A.; Padilla, I., Romero, M., 2022, Mullite production by valorization of a hydrodesulphurization catalyst waste,

[14] Bella, M.L., Hamidouche, M., Gremillard, L. 2021, Preparation of mullite‐alumina composite by reaction sintering between Algerian kaolin and amorphous aluminum hydroxide, Ceram. Int. 47, 16208–16220.

[15] Zhang, C., Liu, F.F., Guo, J.B., Guo, Z.Z., Guo, M., Yang, S.Y., Xu, C.Y., Sun, M.Y., Xu, H., Fang, S.J. 2023, The study on the preparation of ultra‐low thermal expansion ceramic with high elastic modulus, J. Phys.: Conf. Ser. 2478.

[16] Keziz, A., Heraiz, M., Sahnoune, F., Rasheed, M., 2023, Characterization and mechanisms of the phase's formation evolution in sol‐gel derived mullite/cordierite composite, Ceram. Int. 49(20).

[17] Badanoiu, A.-I., Stoleriu, S.-P., Carocea, A.-C., Eftimie, M.-A., Trusca, R., 2025, Influence of synthesis route on composition and main properties of mullite ceramics based on waste, Mater. 18, 1098.

[18] Yang, J., Lei, L., Zhang, J., 2025, Preparation of Alumina Ceramics via a Two‐Step Sintering Process, Materials 18, 1789,

[19] Khodan, A., Nguyen, T.H.N., Kanaev, A., 2024, Mullite synthesis using porous 3D structures consisting of nanofibrils of aluminum oxyhydroxide chemically modified with ethoxysilanes, J. Compos. Sci. 8, 469,

[20] Zhang, X., Zhang, T., Yi, Z., Yan, L., Liu, S., Yao, X., Guo, A., Liu, J., Hou, F., Ceram., 2020, Multiscale mullite fiber/whisker reinforced silica aerogel nanocomposites with enhanced compressive strength and thermal insulation performance, Int. 46, 28561–28568.

[21] González-Lavín, J., Arenillas, A., Rey-Raap, N, 2025, Overcoming scaling

challenges in sol–gel synthesis: A microwave-assisted approach for iron-based energy materials., Microwave, 1(2), 6.

[22] Viswanath, B., Darshankumar, J., Gunapriya, B., Karthi, M., Sankaramoorthy, T., Murugesan, K., 2022, Preparation and characterization of mullite ceramic nano powder for use in nanocomposites, AIP Conf. Proc. 2446, 120001.

[23] Sembiring, S., Simanjuntak, W, Makara, 2012, X-ray Diffraction Phase Analyses of Mullite Derived from Rice Husk Silica, J. Sci. 16(2), 77–82.

[24] Ilić, S., Ivanovski, V.N., Radovanović, Ž, Egelja, A., Kokunešoski, M., Šaponjić, A., 2020, et al. Structural, microstructural and mechanical properties of sintered iron-doped mullite, Mater. Sci. Eng., B 256.

[25] Zhu, H., Zhu, J., López Valdivieso, A., Min, F., Song, S., Wang, H. 2020, Fuel, Effect of frother addition mode on gas dispersion and coal flotation in a downflow flotation column, 273, 117715.